Comparison of AlGaAs and AlInP cladding layers for red edge−emitting lasers

M. Zorn [1)] , H. Wenzel [1)] , A. Knigge [1)] , U. Zeimer [1)] , M. Weyers [1)]
1) Ferdinand−Braun−Insitut fuer Hoechstfrequenztechnik (FBH), Albert−Einstein−Str. 11, D−12489 Berlin, Germany

Introduction

Red edge−emitting lasers are of potential interest e.g. for visible applications, data storage and consumer electronics (e.g. laser printers and scanners). In the wavelength range between 630 nm and 690 nm the laser parameters like threshold current density and efficiency are critical due to the unfavourable material properties in the AlInGaP material system which is required for this wavelength range. Red edge−emitting lasers normally consist of InGaP quantum wells with AlGaInP waveguide layers embedded in AlInP cladding layers [1]. However, growth and processing of AlInP layers is difficult. Especially high p−doping cannot be achieved in AlInP [2].
In our work we investigated the possibilities of increasing the p−doping of AlInP by changing the growth parameters, especially the growth temperature, in metal−organic vapour phase epitaxy (MOVPE). Furthermore, to overcome the problems caused by the AlInP cladding layers, these were replaced by AlGaAs layers. This gives advantages in the laser processing and the possibility of higher p−doping levels [3]. Furthermore, the dopant zinc (Zn) which easily diffuses through the epitaxial structure can then be replaced by carbon (C) in the cladding layer. Optical in−situ monitoring by reflectance anisotropy spectroscopy (RAS) was used during optimisation of the growth process for example at the InGaP/AlInP interface.

Experimental

All epitaxial layer structures presented in this work were grown in an Aixtron 200/4 low−pressure MOVPE system. The sources used include trimethylgallium (TMGa), trimethylaluminum (TMAl), trimethylindium (TMIn), arsine (AsH_3) and phosphine (PH_3). Silicon (Si) from Si_2H_6 was used for n−doping. Zinc (Zn) from dimethylzinc (DMZn) and carbon (C) from tetrachlorbromide (CBr_4) were utilized for p−doping. The growth pressure was 150 hPa and the main growth temperature was 770°C. Epiready n+ GaAs (100) substrates misoriented 6° towards [111]A were used.
The MOVPE system is equipped with low−strain UV transparent viewports for normal incidence optical access and with a corresponding hole in the liner−tube. In−situ measurements were performed using a LayTec EpiRAS−200 spectrometer that allows combined reflectance anisotropy spectroscopy (RAS) [4,5] and reflectance (R) measurements under standard device growth conditions [6].

Growth Optimization

Fig. 1 shows a complete RAS fingerprint taken during growth of a red laser structure with AlInP cladding layers. This fingerprint (also called colorplot) was obtained by taking RAS spectra in the range between 1.5 eV (826 nm) and 5 eV (248 nm) continously. Afterwards the spectra are color−coded and plotted versus growth time [6]. The different growth stages (deoxidation etc.) as well as the growth of the different layers with their correspondig composition and doping levels can clearly be distinguished. Failures in the growth process can be identified easily and the reproducibility can be checked by simply comparing the fingerprints of different growth runs. Fig. 2 shows two transients taken at 3.8 eV (326 nm) in time−resolved mode during growth of two different laser structures. Here also the growth of the layers with their correspondig doping level can clearly be distinguished. The RAS signal behaves as reported earlier [7,8]: for n−type doping the RAS signal decreases while p−type doping leads to an increase in the RAS signal at this photon energy (wavelength). Furthermore, it can be seen that during growth of the first laser structure (dashed line) the RAS signal shows a strong increase up to 36 RAS units during heating of the n:InGaP from 600°C up to 770°C (grey circle). This is a sign for surface roughening due to phosphorus desorption.

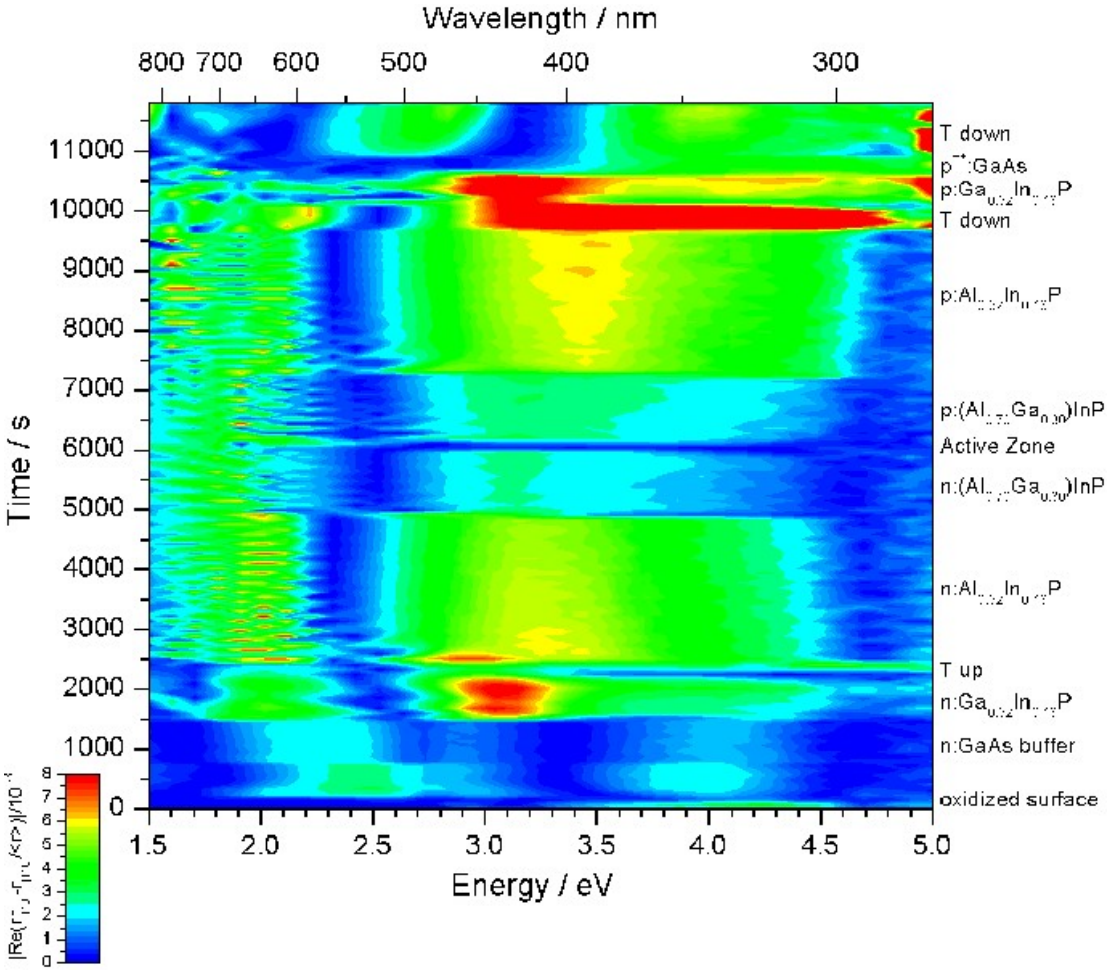

Fig. 1: *Typical RAS fingerprint (colorplot) taken during growth of a red laser structure. The different growth stages and layers with their correspondig doping types and levels can clearly be distinguished.*

The second laser grown with an optimised procedure shows only a small increase in the RAS signal up to 5 RAS units at the n:InGaP/n:AlGaInP interface. This shows that in this case nearly no surface degradation has occured at this interface. Ex−situ microscope measurements support these results: The first sample showed a bad morphology while the second sample is mirror−like.

When growing laser structures using AlGaAs cladding layers, phosphorus desorption is not a problem because no InGaP layer is needed between the GaAs and the AlInP to reduce the band offsets. In the AlGaAs system the same effect can be achieved more easily by introducing a graded index layer between the GaAs and the AlGaAs layer.

The doping profiles of the different laser structures where investigated by SIMS. Fig. 3 shows doping profiles of laser structures with Zn:AlInP cladding layers and for comparison with Zn:AlGaAs cladding layers. It can be seen that the p−doping level in the AlGaAs is much higher than in the AlInP grown at 770°C. The achivable p−doping level in AlInP can be increased by lowering the growth temperature. At a growth temperature of 660°C the Zn concentration is comparable to the one in AlGaAs. However, the growth of AlInP at lower growth temperatures leads to a reduced crystal quality. Furthermore, the higher Zn incorporation at 660°C in AlInP obviously leads to a higher Zn diffusion in the waveguide layer. When lowering the growth temperature, broad area devices show a decrease of the threshold current density and an increase of the differential efficiency. In the lasers with AlGaAs cladding layers a strong improvement can be achieved by replacing Zn by C from CBr_4 in the p:AlGaAs layer. Due to the reduced Zn diffusion the threshold current density decreases and the differential effiency inceases.

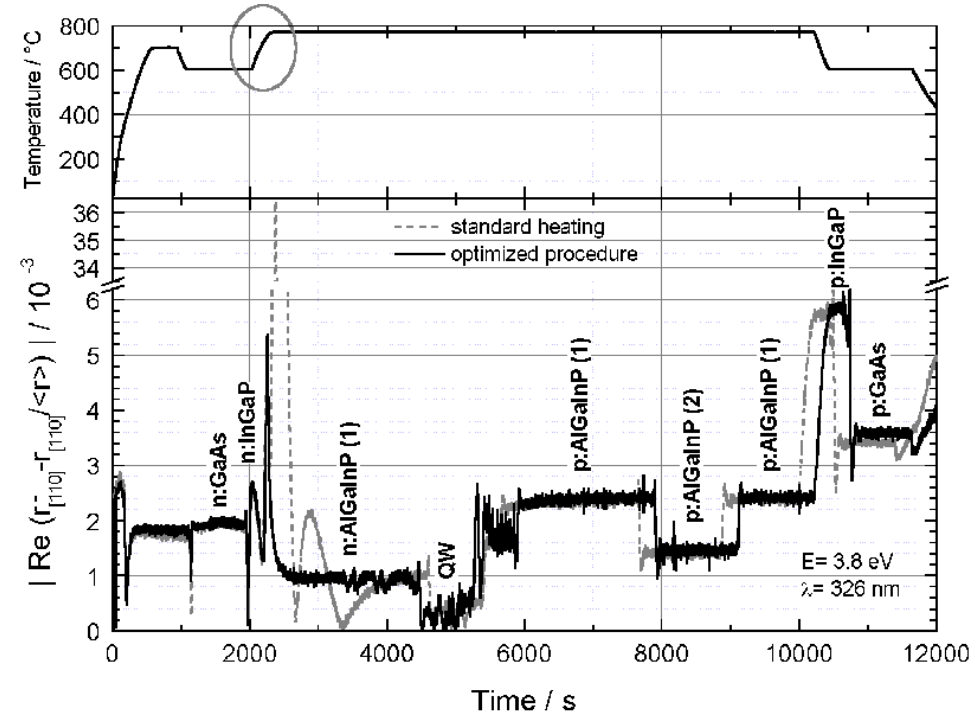

Fig. 2: *RAS transients taken at 3.8 eV (326 nm) during growth of two different red laser structures (lower part). The grown layers are indicated. The upper part shows the respective growth temperature.*

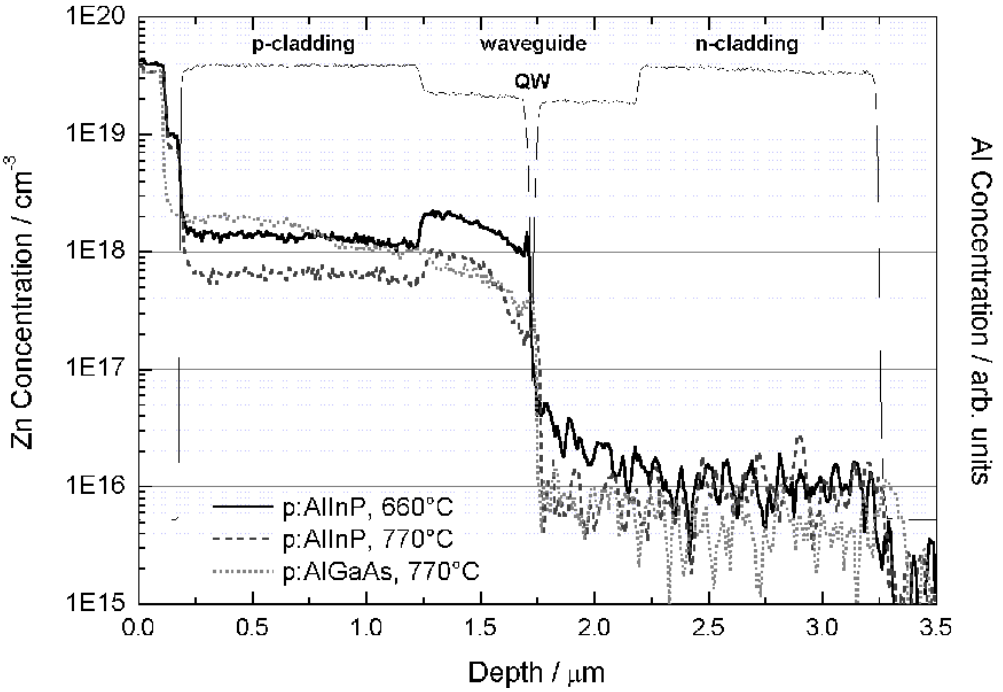

Fig. 3: *SIMS profiles showing the Zn incoorporation in the laser structures with: a) Zn:AlInP cladding layers grown at 660C, b) Zn:AlInP cladding layers grown at 770C, c) Zn:AlGaAs cladding layers grown at 770C.*

As result of the optimization process we focused on two different layer structures for the growth of the laser structures: One with AlInP cladding layers using Zn and a growth temperature of 660°C on the p−side and one consisting of AlGaAs using C for p−type doping grown at 770°C.

Laser Data

For the growth of laser structures we used compressively strained double quantum wells for an emission wavelength of 653 nm. In pulsed operation our lasers with AlInP cladding layers show a low threshold current density of 530 A/cm^2 with an external differential efficiency of 69% for 100 µm x 1000 µm stripes which seems to be comparable to results reported in the literature [9,10]. For lasers containing AlGaAs cladding layers we obtained a threshold current density of 590 A/cm^2 and an external differetial efficiency of 77 % under the same conditions. Due to the different optical properties the lasers with AlGaAs cladding layers have a reduced vertical far field angle of 30° in comparison to 36° for the lasers with AlInP cladding layers. Therefore, it should be pointed out that although the vertical far field angle is reduced (resulting in a smaller quantum well confinement factor) the threshold current density increases only slightly. Furthermore, the external differential efficiency is even higher. Coated low mesa stripe lasers fabricated from layer structures with AlGaAs cladding layers using carbon doping on the p−side achieved an output power of about 0.5 W at 650 nm and 20°C in cw operation.

In summary, replacing the Zn:AlInP cladding layers bei C:AlGaAs seems to be a promising way to grow high−power red laser structures. However, further investigations (e.g. life time tests) have to be carried out to prove this assumption.

References

[1] D.P. Bour, R.S. Geels, D.W. Treat, T.L. Paoli, F. Ponce, R.L. Thornton, B.S. Krusor, R.D. Bringans, D.F. Welch, IEEE J. Quant. Electron. ***30*** (1994) 593

[2] Y. Nishikawa, Y. Tsuburai, C. Nozaki, Y. Ohba, Y. Kokubun, H. Kinoshita, Appl. Phys. Lett. ***53*** (1988) 2182

[3] P. Unger, G.−L. Bona, R. Germann, P. Roentgen, D.J. Webb, IEEE J. Quant. Electron. ***29*** (1993) 1880

[4] D.E. Aspnes, Mater. Sci. Eng. B ***30*** (1995) 109

[5] J.−T. Zettler, K. Haberland, M. Zorn, M. Pristovsek, W. Richter, P. Kurpas, M. Weyers, J. Cryst. Growth ***195*** (1998) 151

[6] K. Haberland, P. Kurpas, M. Pristovsek, J.−T. Zettler, M. Weyers, W. Richter, Appl. Phys. A ***68*** (1999) 309

[7] K. Haberland, A. Bhattacharya, M. Zorn, M. Weyers, J.−T. Zettler, W. Richter, J. Electron. Mater. ***29*** (2000) 468

[8] M. Zorn, K. Haberland, A. Knigge, A. Bhattacharya, M. Weyers, J.−T. Zettler, W. Richter, J. Cryst. Growth ***235*** (2002) 25

[9] S. Orsila, M. Toivonen, P. Savolainen, V. Vilokkinen, P. Melanen, M. Pessa, SPIE ***3628*** (1999) 203

[10] P. Raisch, R. Winterhoff, W. Wagner, M. Kessler, H. Schweizer, T. Riedl, R. Wirth, A. Hangleitner, F. Scholz, Appl. Phys. Lett. ***74*** (1999) 2158